Chiral differentiation of the noscapine and hydrastine stereoisomers by electrospray ionization tandem mass spectrometry

Tibor Nagy[1], Ákos Kuki[1], Borbála Antal[1], Lajos Nagy[1], Mihály Purgel[2], Attila Sipos[3], Miklós Nagy[1], Miklós Zsuga[1], Sándor Kéki[1]*

[1]*Department of Applied Chemistry, University of Debrecen, Hungary,*
[2]*MTA-DE Homogeneous Catalysis and Reaction Mechanisms Research Group*
[3]*Department of Pharmaceutical Chemistry, University of Debrecen, Hungary*

* Corresponding author: keki.sandor@science.unideb.hu, tel: +36 52 518662/22455; fax: +36 52 518662; *H-4032 Debrecen, Hungary*

Abstract

Energy dependent collision-induced dissociation (CID) of the dimers $[2M+Cat]^+$ of the noscapine and hydrastine stereoisomers was studied where Cat stands for Li^+, Na^+, K^+ and Cs^+ ions. These dimers were generated "in situ" from the electrosprayed solution. The survival yield (SY) method was used for distinguishing the noscapine and hydrastine dimers. Significant differences were found between the characteristic collision energies (CE_{50}, i.e. the collision energy necessary to obtain 50% fragmentation) of the homo- (R,R; S,S) and heterochiral (R,S; S,R) stereoisomers. To distinguish the enantiomer pairs L-, D-tyrosine ($[M+Tyr+Cat]^+$) and L-, D-lysine ($[M+Lys+Cat]^+$) were used as chiral selectors. Furthermore, these heterodimers $[M+amino\ acid+Cat]^+$ were also applied to determine the stereoisomeric composition. It was found that the characteristic collision energy (CE_{50}) of the noscapine and hydrastine homodimers ($[2M+Cat]^+$) was inversely proportional to the ionic radius of the cations. Furthermore, the activation energy of fragmentation of the noscapine and hydrastine dimers was also estimated using a simple collision model and supported by high level quantum chemical calculations.

Keywords: noscapine, hydrastine, chiral differentiation, survival yield, stereoisomers, chiral mass spectrometry

Introduction

Noscapine is an isoqiunoline alkaloid derived from opium. Noscapine has medical benefits [1,2], it has been used as a natural antitussive agent for decades without any toxic effects. Furthermore, this alkaloid shows antitumor activity in various cancers like breast, lung and colon cancer [3-7]. Noscapine has two chirality centres at the positions of C(3) and C(5'), resulting in four stereoisomers of this compound of which, however, only one stereoisomer, the **(-)-**α-noscapine can be found in nature. The other noscapine isomers can be prepared by synthetic methods.

Hydrastine is another natural alkaloid with similar structure to that of the noscapine. The only difference is the lack of the methoxy group at the C(4') position. All of the hydrastine isomers are encountered in different plants, however, the synthesis of these isomers is also known. The chemical structures of noscapine and hydrastine are presented in Scheme 1.

Scheme 1

In general, the enantiomers have different effects on the human body [8,9]. Sometimes, the enantiomers can show adverse effects, therefore, the separation and identification of the enantiomers are crucial. Several methods have been developed using mass spectrometry to identify the stereoisomers and to determine the enantiomeric composition. The enantiomers can be distinguished using chiral selectors by forming diasteroisomers. The chiral mass spectrometric methods can be divided into five basic groups [10]: the kinetic method [11], the host-guest method [12-14], the ion/molecule equilibrium method [15], the CID method [16,17] and the ion mobility spectrometry method [18,19]. The CID mass spectrometric methods for chiral recognition are working with chiral selectors, and using the intensity ratios at defined collision energy as the source of the chiral information.

In this paper, a novel tandem mass spectrometric approach for the differentiation of the stereoisomers of both noscapine and hydrastine in the presence and in the absence of chiral selectors by applying the survival yield (SY) method is presented. One of the main advantages of the SY method compared to a common CID method is that the survival yield curves are constructed based on the intensity ratios at more, different collision energies which can produce more accurate results. Furthermore, based on the SY method the activation parameters can also be estimated [20].

The fragmentations of the homodimers formed and the ones with chiral selector were studied. As chiral selector the L,D-lysine and the L,D-tyrosine were used since the pure amino acids and their derivatives are easily available. Furthermore, the chiral recognitions of the amino acids were achieved by many methods [11, 21] that suggest the amino acids can be used as universal chiral selectors.

Experimental

Chemicals

Noscapine and hydrastine stereoisomers were synthesized as described in Ref [22, 23]. The different stereoisomers are labelled with numbers as it can be seen in Scheme 1. The D-tyrosine was purchased from Sigma Aldrich (St. Louis, United States). L-, D-lysine and the L-tyrosine from Reanal (Budapest, Hungary) and methanol from VWR Radnor (United States) were used without further purification. Lithium, sodium, potassium and caesium chloride were obtained from Sigma Aldrich (St. Louis, United States).

Sample preparation

Noscapine and hydrastine were dissolved in methanol at a concentration of 0.025 mM. The concentration of the chiral selector was five times higher than those of noscapine and hydrastine. To obtain the corresponding adducts LiCl, NaCl, KCl and CsCl were added to the noscapine and hydrastine solutions to obtain 2 mM concentration of the salts.

Electrospray Quadrupole Time-of-Flight MS/MS (ESI-Q-TOF)

A MicroTOF-Q type Qq-TOF MS instrument (Bruker Daltonik, Bremen, Germany) was used for the MS/MS measurements. The instrument was equipped with an electrospray ion source where the spray voltage was 4 kV. N_2 was utilized as drying gas. The drying temperature was 180 °C and the flow rate was 4.0 L/min. For the MS/MS experiments, nitrogen was used as the collision gas and the collision energies were varied in the range of 1-39 eV (in the laboratory frame). The pressure in the collision cell was determined to be 1.2×10^{-2} mbar. The precursor ions for MS/MS were selected with an isolation width of 4 *m/z* units. The mass spectra were recorded by means of a digitizer at a sampling rate of 2 GHz. The spectra were evaluated with the DataAnalysis 3.4 software from Bruker.

Determination of the survival yield (SY) and the characteristic collision energy (CE_{50})

The efficiency of the fragmentation was determined quantitatively by the survival yield method (SY). The experimental SY curves were built according to equation 1:

$$SY = \frac{I_p}{I_p + \sum I_f} \qquad (1)$$

where I_p and $\sum I_f$ are the intensity of the precursor ion and the sum of all fragment ion intensities, respectively. Additionally, the SY curve can be described by a two-parameter sigmoid function [24] based on equation 2.

$$SY = \frac{1}{1 + a\, e^{bCE}} \qquad (2)$$

where a and b are constants and CE is the laboratory frame collision energy. These constants (a and b) were determined by fitting the calculated curve to the measured one applying a spreadsheet software. The value of the collision energy at SY=0.5 (CE_{50}) can be expressed by eq. 3. using the parameters of eq. 2.

$$CE_{50} = \frac{\ln(1/a)}{b} \qquad (3)$$

Based on eight independent measurements the confidence interval of the CE_{50} value determination is ±0.007 eV at 95% significance level.

Estimation of the activation energy of the fragmentation

A simple collision model was used to estimate the activation energy (E_o) of the fragmentation of noscapine and hydrastine dimers [20]. The model computes the internal and kinetic energy changes in a quadrupole type mass spectrometer. Using the Rice–Ramsperger–Kassel (RRK) theory the internal energy dependent rate constant of the fragmentation can be determined. The model was used for the construction of the SY curves. Fitting the calculated SY curve to the measured one the activation energy of the fragmentation can be estimated. The parameters of the collision model were determined using Leucine enkephaline as a “calibrant”. The collision cross-sections were estimated by scaling it by the mass ratio of the noscapine and hydrastine dimers to Leucine enkephaline. The numbers of effective oscillators was proportioned by the degrees of freedom (DOF). The energy transfer efficiency was kept constant as obtained for Leucine enkephaline.

Quantum chemical calculations

Density Functional Theory (DFT) calculations were performed by the B3LYP exchange-correlation functional [25] where 6-31+G(d) were the standard split-valence basis sets [26]. For the alkali metal ions we have chosen the Ermler–Christiansen relativistic effective core potential (RECP) basis set [27-29]. Geometry optimizations were carried out *in vacuum*. The relative energies are Gibbs free energies obtained by frequency analysis. All of these calculations were carried out using the Gaussian 09 software package [30]. The lack of imaginary frequencies in vibrational spectral calculations was taken to verify that the calculated stationary points on the potential energy surfaces (PES) represented true minimal.

Results and discussion

Differentiation of the dimers of the stereoisomers

The collision induced dissociations (CID) of the noscapine and hydrastine dimers $[2M+Cat]^+$ were studied using sodium, potassium and caesium ions as the cationizing agents. These stereoisomeric dimers were generated "in situ" under electrospray conditions. The formation of this type of noncovalent dimers is specific to the ESI [31,32]. Fig. 1 shows the MS/MS spectrum of the sodiated noscapine 1 (R,S) dimers produced under ESI-conditions.

Fig. 1.

The *m/z* 436 product ion was identified as the single, sodiated noscapine ($[M+Na]^+$). In the MS/MS spectrum of the sodiated noscapine **1** (R,S) homodimer ($[2M+Na]^+$), only the sodiated noscapine ion ($[M+Na]^+$) appeared as the product ion. The same fragmentation was observed in the case of hydrastine homodimers. The MS/MS spectra of the potassiated and ceasiated dimers are similar to those of the sodiated ones presented in Fig. 1. Therefore the fragmentations of the homodimers are considered as simple unimolecular dissociations. The lithiated homodimers were also studied. However, these homodimers suffer fragmentation before the dissociation of the dimers. Thus, the energetics of the fragmentation of the lithiated homodimers cannot be compared to those of the sodiated, potassiated and the ceasiated homodimers. The results of the study of the lithiated homodimers are therefore presented in the supplementary information. To study the energy dependent dissociation of the dimers the SY curves were constructed. The SY curves of the sodiated noscapine (a) and hydrastine (b) dimers are presented in Fig. 2.

Fig. 2.

As seen in Fig. 2, significant difference can be found between the SY plots of the sodiated dimers of the noscapine stereoisomers compared to those of the hydrastine stereoisomers. The survival yield curves of the sodiated hydrastine enantiomers are closer to each other than those of the noscapine enantiomers as it can be seen in Fig. 2 insets. The characteristic collision energies (CE_{50}) were determined from the SY curves. Table 1 shows the CE_{50} values and the normalized CE_{50} values of the noscapine and hydrastine dimers using different cations.

Table 1.

As Table 1 shows, less difference can be found between the characteristic collision energies of the homodimers generated from the enantiomers than between those of the epimers. However, based on the normalized characteristic collision energies in every case, the suitable ionized homodimers can be found for the differentiation. Furthermore, all of the stereoisomers can be ordered based on their normalized characteristic collision energies. With the help of this determined order the stereoisomers can be identified. As an example it was found that the CE_{50} values for the sodiated dimers of the noscapine ($[2M+Cat]^+$) stereoisomers decrease in the order of noscapine **1** (R,S) > noscapine **2** (S,R) >noscapine **3** (R,R) > noscapine **4** (S,S).

Distinction of the stereoisomers with chiral selectors

The dimers of the amino acid - noscapine and hydrastine stereoisomers are generated "in situ" in the electrospray ion-source. The fragmentations of the four stereoisomers of noscapine-amino acid and hydrastine-amino acid dimers were also studied using collision energy dependent CID MS/MS. These mixed dimers required lower collision energies to reach the same extent of fragmentation as the corresponding homodimers. The MS/MS spectra of the sodiated noscapine **3**, (R,R)-L-tyrosine dimers are presented in Fig. 3. Beside the precursor ion only the sodiated single noscapine appeared in the MS/MS spectra like it was in the case of the homodimers. The results of the lithiated homodimers can be found in the supplementary information. Similar fragmentation patterns were observed for hydrastine and using lysine as the chiral selector.

Fig. 3.

Neither the cationized L-, D-lysine nor the L-, D-tyrosine has appeared in the MS/MS spectra, indicating that noscapine and hydrastine have higher affinity to the sodium ion than to the amino acids. Using the SY curves obtained by energy dependent CID experiments the CE_{50} values of all of the heterodimers were determined. The SY plots of the sodiated dimers of the noscapine stereoisomers and L-tyrosine are shown in Fig. 4.

Fig. 4.

Fig. 4 shows that significantly larger shift can be found between the survival yield curves of the heterodimers than between those of the homodimers. Furthermore, the heterodimers need significantly lower collision energies to reach the same extent of fragmentation. The potassiated and the ceasiated heterodimers cannot be studied because these dimers suffer fragmentation under even the lowest collision energy.

The normalized CE_{50} values of the heterodimers are presented in Table 2. The noscapine-tyrosine and noscapine-lysine dimers have similar CE_{50} values in spite of the fact that the lysine has fewer degrees of freedom (DOF). It may suggest that the binding energy of the cation to the amino acid is higher in the case of noscapine-lysine dimers. In addition, higher differences in the CE_{50} values can be found for the sodiated heterodimers involving tyrosine than for those involving the lysine.

Table 2

The heterodimers have considerably lower CE_{50} values than the homodimers but the differences between the stereoisomers are significantly larger.

The cross-chiral effect [33] appeared as it can be seen in the CE_{50} values of the heterodimers, using the D-amino acids the order of CE_{50} values is the opposite between the enantiomers compared to the dimers with L-amino acids. For example, the order of the CE_{50} values for the sodiated noscapine- L-tyrosine ($[M+L\text{-}Tyr+Na]^+$) is: noscapine **1** (R,S) > noscapine **2** (S,R) > noscapine **4** (S,S) > noscapine **3** (R,R). On the contrary, using D-tyrosine the order is altered as follows: noscapine **2** (S,R) > noscapine **1** (R,S) > noscapine **3** (R,R) > noscapine **4** (S,S). Despite the inversion of the CE_{50} values of the enantiomers, the difference between the epimers is similar. This inversion can help in the identification of the stereoisomers.

Determination of the stereoisomeric composition

The stereoisomeric excess (se%) and the stereoisomeric purity (sp%) were calculated using equation 4 and 5, respectively.

$$\text{se\%} = \frac{100(S_1 - S_2)}{(S_1 + S_2)} \qquad (4)$$

$$\text{sp\%} = \frac{se\% + 100}{2} \qquad (5)$$

where S_1 and S_2 indicate the amounts of two different stereoisomers.

To determine the stereoisomeric composition, the heterodimers were studied since the differences between the CE_{50} values of the stereoisomers are more significant than in the case of the homodimers. As an example Fig. 5 shows the characteristic collision energy of the hydrastine **2** (S,R) and hydrastine **3** (R,R) mixtures as a function of the stereoisomeric excess (a) and the stereoisomeric purity (b). L-tyrosin and sodium were used as the chiral selector and the ionizing agent, respectively. As can be seen in Fig. 5, linear correlation was found between the stereoisomeric excess / stereoisomeric purity and the characteristic collision energy, allowing to use this correlation as a calibration curve for the determination of the stereoisomeric composition.

Fig. 5.

Mixtures for calibration were made from standard samples with known stereoisomeric composition. Two different calibration series were used to check the validity of the calibration. The two calibration series were measured on two different days. The differences between the corresponding CE_{50} values are less than 2.5 %. To test the calibration curve validity, mixtures with different stereoisomeric composition were measured. These test mixtures were measured three times. Table 3 contains the composition of the test solutions, the measured and calculated stereoisomeric purity of the hydrastine **2** (S,R) and the standard deviation of the stereoisomeric purity.

Table 3

The measured stereoisomeric purity of the test mixtures are in good agreement with the calculated data. The results show that the stereoisomeric purity can be determined with good accuracy in the full range.

Estimation of the activation energy of the fragmentation of the homo- and hetorodimers

In further experiments, the activation energy of the fragmentation (E_o) was calculated, as it was described in the experimental section. As seen in Figs. 1 and 3, only one product ion, i.e. the cationized noscapine ($[M+Cat]^+$) appeared in the MS/MS spectra of the dimers. Hence, the activation energy of the dissociation of the dimers in the gas phase can be estimated. The calculated E_o values and the corresponding pre-exponential factors are presented in Table S6-S8 in the Supplementary Information. As seen in the tables, the sodiated homodimers have the highest activation energy. Furthermore, as it can be expected, .parallel with the increase of the cation size the activation energy of the fragmentation is decreasing.

For the activation energy of the fragmentation of the sodiated noscapine ($[M+Na]^+$) a value of 1.11 eV was calculated. For the sodiated heterodimers the activation energy of the fragmentation was calculated to be around 0.5 eV. Therefore, the sodiated heterodimers dissociate at significantly lower collision energy than the sodiated noscapine. It suggests that the sodiated heterodimers are fragmented before the single sodiated noscapine, as it can be seen in the MS/MS spectrum of the sodiated heterodimers in Fig. 3.

It should be noted, that with the use of different cations the CE_{50} values of the noscapine and hydrastine homodimers can be altered in a wide range. Values of CE_{50} decrease with the ionizing cation size which is in line with the charge density of the ions. Figs. S8 and S9 in the Supplementary Information show the calculated CE_{50} values of the noscapine and hydrastine homodimers ($[2M+Cat]^+$) as a function of the reciprocal of the ionic radius of the cation. As it can be seen in Figs. S8 and S9, linear correlation was found between the CE_{50} values and the reciprocal of the ionic radius. Table 4 shows the slopes, the intercepts and the correlation coefficients of the linear trend lines of the CE_{50} *versus* reciprocal ionic radius for the noscapine and hydrastine homodimers.

Table 4

As Table 4 shows, very good correlations were obtained, and the slopes and the intercepts are similar for all the trend lines.

Furthermore, closely linear correlation was also found between the estimated activation energy of the fragmentation of the noscapine and hydrastine homodimers ($[2M+Cat]^+$) and the reciprocal of the ionic radius of the ionizing cation. As examples, Fig. 6 shows the activation energy values of the fragmentation of noscapine **1** (R,S) and hydrastine **4** (S,S) homodimers as a function of the reciprocal of the ionic radius of the cation.

Fig. 6.

The correlations presented in Fig. 6 reflect that the smaller cations have higher charge density, creating stronger bonds.

Quantum chemical calculations

To obtain more information on the structure and the energetics of the homodimers high level quantum chemical calculations were carried out. The density functional theory (DFT) calculations were performed on the dimers of noscapine **1** (R,S) and noscapine **4** (S,S) cationized with Na^+, K^+ and Cs^+ ions. The most stable $[M+Cat]^+$ was generated by the coordination of the alkali metal ions to the oxo group at C1 and the methoxy group at C7. The coordination of the alkali metal ions are the same for all cationized noscapines. The calculated structures of the dimers are shown in Fig. 7.

Fig. 7.

As seen in Fig. 7, the calculated structures for the cationized noscapine dimers ($[2M+Cat]^+$) depend significantly on the cation. The sodiated noscapine dimers possess square planar geometry. On the contrary, potassiated and caesiated noscapine dimers reveal pyramidal arrangement. The structure of the potassiated noscapine dimer is a distorted pyramid, while the caesiated noscapine dimer reveals also pyramidal structure, however, with less distortion. Based on the DFT calculations the activation and the Gibbs free energies were determined for the dissociation channel of eq. 6.

$$[2M + Cat]^+ \rightarrow [M + Cat]^+ + [M] \qquad (6)$$

The Gibbs free energies and the estimated activation energies for the above process (eq. 6.) are presented in Table 5.

Table 5

According to the data of Table 1, both the DFT calculation and the estimated activation energy values show that the dimers of noscapine **1** (R,S) require higher energy for the fragmentation than those of noscapine **4** (S,S). Furthermore, both the Gibbs free energy calculated by DFT and the estimated activation energy values decrease with the increasing size of the cation. Thus, the trends and the values of the activation energies for the fragmentation are in good agreement with the calculated Gibbs free energies.

Conclusions

Noscapine and hydrastine stereoisomers with two chirality centres were distinguished on the basis of the energetics of the fragmentation using tandem mass spectrometry. The dimers of the stereoisomers which were generated in the ESI ion-source were studied. Based on the order of the CE_{50} values of the homodimers the stereoisomers can be identified. Beside the homodimers, the dimers of noscapine and hydrastine with amino acids were also investigated. With the use of the chiral selectors the difference between the CE_{50} values increases and further information can be obtained about the stereoisomeric composition, which can be determined with good accuracy.

Furthermore, the activation energies of the fragmentations were estimated. The activation energies of the fragmentations of the single sodiated noscapine ($[M+Na]^+$) and the sodiated noscapine heterodimers were found to be different around 0.5 eV which explains, why the MS/MS spectrum of the sodiated noscapine heterodimers shows only one product ion originated from the fragmentation of the heterodimers of the noscapine. In addition, linear correlation was found between the CE_{50} values and the reciprocal of the ion radius of the cation, which are in good agreement with the result of DFT calculations.

It can be concluded that our tandem mass spectrometric method is capable of identifying the noscapine and hydrastine stereoisomers and determining the stereoisomeric composition. In addition, this tandem mass spectrometric approach can be extended to other classes of stereoisomeric compounds.

Acknowledgement

The work reported here was supported by the grant K-101850 given by OTKA (National Found for Scientific Research Development, Hungary), and the TÁMOP-4.2.2.A-11/1/KONV-2012-0036 project co-financed by the European Union and the European Social Fund. This work was also supported by the European Union and the State of Hungary, co-financed by the European Social Fund in the framework of TÁMOP-4.2.4.A/ 2-11/1-2012-0001 'National Excellence Program' (S. K.) and European Union and the European Social Fund through project Supercomputer, the National Virtual Lab, grant no.: TÁMOP-4.2.2.C-11/1/KONV-2012-0010.

References

[1] S. Zughaier, P. Karna, D. Stephens,R. Aneja. Potent anti-inflammatory activity of novel microtubule-modulating brominated noscapine analogs. 2010, PLoS ONE, 5 (2) e9165.

[2] M. Mahmoudian, N. Mojaverian. Effect of noscapine, the antitussive opioid alkaloid, on bradykinin-induced smooth muscle contraction in the isolated ileum of the guinea-pig. Acta. Physiol. Hung. 2001, 88, 231.

[3] M. Mahmoudian, P. Rahimi-Moghaddam. The Anti-Cancer Activity of Noscapine: A Review. Recent. Pat. Anti-Canc. 2009, 4, 92.

[4] N. Jhaveri, H. Cho, S. Torres,W. Wang, A. H. Schönthal, N. A. Petasis, S. G. Louie, F. M. Hofman, T. C. Chen,. Noscapine inhibits tumor growth in TMZ-resistant gliomas. Cancer Lett. 2011, 312, 245.

[5] W. Su, L. Huang, Q. Ao, Q. Zhang, X. Tian, Y. Fang, Y. Lu,. Noscapine sensitizes chemoresistant ovarian cancer cells to cisplatin through inhibition of HIF-1a. Cancer Lett. 2011, 305, 94.

[6] Z. Yang, M. Liu, X. Peng, X. Lei, L. Zhang, W. Dong. Noscapine induces mitochondria-mediated apoptosis in human colon cancer cells in vivo and in vitro. Biochem. Bioph. Resh. Co. 2012, 421, 627.

[7] M. Chougule, M. R. Patel, R. Sachdeva, T. Jackson, M. Singh. Anticancer activity of Noscapine, an opioid alkaloid in combination with Cisplatin in human non-small cell lung cancer. Lung Cancer. 2011, 71, 271.

[8] Jr. J. R. Holtman, P. A. Crooks, J. K. Johnson-Hardy, M. Hojomat, M. Kleven, E. P. Wala. Effects of norketamine enantiomers in rodent models of persistent pain. Pharmacol. Biochem. Be. 2008, 90, 676.

[9] Jr. W. R. Henderson, E. R. Banerjee, E. Y. Chi. Differential effects of (S)- and (R)-enantiomers of albuterol in a mouse asthma model. J. Allergy. Clin. Immun. 2005, 116, 332.

[10] L. Wu,F. G. Vogt. A review of recent advances in mass spectrometric methods for gas-phase chiral analysis of pharmaceutical and biological compounds. J. Pharm. Biomed. Anal. 2012, 69, 133.

[11 L. Wu, W. Andy Tao, R. G. Cooks. Kinetic method for the simultaneous chiral analysisof different amino acids in mixtures. J Mass Spectrom. 2003, 38, 386.

[12] A. R. M. Hyyryläinen, J. M. H. Pakarinen, P. Vainiotalo, G. Stájer, F. Fülöp. Diastereochemical Differentiation of β-Amino Acids Using Host–Guest Complexes Studied by Fourier Transform Ion Cyclotron Resonance Mass Spectrometry. J. Am. Soc. Mass Spectrom. 2007, 18, 1038.

[13] M. Vincenti, A. Irico. Gas-phase interactions of calixarene- and resorcinarene-cavitands with molecular guests studied by mass spectrometry. Int. J. Mass Spectrom. 2002, 214, 23.

[14] M. Shizuma, M. Ohta, H. Yamada, Y. Takai, T. Nakaoki, T. Takeda, M. Sawada. Enantioselective complexation of chiral linear hosts containing monosaccharide moieties with chiral organic amines, Tetrahedron. 2002 58, 4319.

[15] A. R. M. Hyyryläinen, J. M. H. Pakarinen, E. Forró, F. Fülöp, P. Vainiotalo. Chiral Differentiation of Some Cyclopentane and Cyclohexane β-Amino Acid Enantiomers Through Ion/Molecule Reactions. J. Am. Soc. Mass Spectrom. 2009, 20, 1235.

[16] S. P. Gaucher, J. A. Leary. Influence of metal ion and coordination geometry on gas phase dissociation and stereochemical differentiation of N glycosides. Int. J. Mass Spectrom. 2000, 197, 139.

[17] C-T. Yu, Y-L. Guo, G-Q. Chen, Y-W. Zhong. Recognition of Zinc(II) Ion Complexes Composed of Bicyclo[3.3.0] Octane-2,6-Diol and s-Naproxen Probed by Collisional-Induced Dissociation. J. Am. Soc. Mass Spectrom. 2004, 15, 795.

[18] K. Giles, J. L. Wildgoose, D. J. Langridge, I. Campuzano. A method for direct measurement of ion mobilities using a travelling wave ion guide. Int. J. Mass Spectrom. 2010, 298, 10.

[19] V. Domalain, V. Tognetti, M. Hubert-Roux, C. M. Lange, L. Joubert, J. Baudoux, J. Rouden, C. Afonso. Role of Cationized and Multimers Formation for Diastereomers Differentation by Ion Mobility-Mass Spectrometry. J. Am. Soc. Mass Spectrom. 2013, 24, 1437.

[20] Á. Kuki, G. Shemirani, L. Nagy, B. Antal, M. Zsuga, S. Kéki. Estimation of Activation Energy from the Survival Yields: Fragmentation Study of Leucine Enkephalin and Polyethers by Tandem Mass Spectrometry. J. Am. Soc. Mass Spectrom. 2013, 24, 1064.

[21] Z-P. Yao, T. S. M. Wan, K-P. Kwong, C-T. Che. Chiral analysis by electrospray ionization mass spectrometry/mass spectrometry. 1. Chiral recognition of 19 common amino acids. Anal. Chem. 2000, 72, 5383.

[22] Gy. Gaál, P. Kerekes, R. Bognár. About the accompanying alkaloids of morphine VI. Preparation of the narcotine isomers. J. Praktisch. Chem. 1971, 313, 935.

[23] P. Kerekes, Gy. Gaal, R. Bognar. Elimination of phenolic hydroxyl group: Conversion of (-)-α-narcotine into (-)-β-hydrastine. Acta. Chim. Hung. 1980, 103, 339.

[24] T. M. Kertesz, L. H. Hall, D. W. Hill, D. F. Grant. CE50: Quantifying Collision Induced Dissociation Energy for Small Molecule Characterization and Identification. J. Am. Soc. Mass Spectrom. 2009, 20, 1759.

[25] Y. Zhao, D. G. Truhlar. The M60 suite of density functional for main group thermochemistry, thermichemical kinetics, noncovalent interactions, excited states, and

transition elements: two new functionals and systematic testing of four M60-class functional and12 other functional. Theor. Chem. Acc. 2008, 120, 215.

[26] W. J. Hehre, R. Ditchfield, J. A. Pople. Self—Consistent Molecular Orbital Methods. XII. Further Extensions of Gaussian—Type Basis Sets for Use in Molecular Orbital Studies of Organic Molecules. J. Chem. Phy. 1972, 56, 2257.

[27] L. F. Pacios, P. A. Christiansen. Ab initio relativistic effective potentials with spin-orbit operators. I. Li through Ar. J. Chem. Phys. 1985, 82, 2664.

[28] M. M. Hurley, L. F. Pacios, P. A. Christiansen. Ab initio relativistic effective potentials with spin-orbit operators. II. K through Kr. J. Chem. Phys. 1986, 84, 6840.

[29] R. B. Ross, J. M. Powers, T. Atashroo, W. C. Ermler, L. A. LaJohn, P. A. Christiansen. Ab initio relativistic effective potentials with spin–orbit operators. IV. Cs through Rn, R. B. Ross. J. Chem. Phys. 1990, 93, 6654.

[30] M. J. Frisch, G. W. Trucks, H. B. Schlegel, G. E. Scuseria, M. A. Robb, J. R. Cheeseman, G. Scalmani, V. Barone, B. Mennucci, G. A. Petersson, H. Nakatsuji, M. Caricato, X. Li, H. P. Hratchian, A. F. Izmaylov, J. Bloino, G. Zheng, J. L. Sonnenberg, M. Hada, M. Ehara, K. Toyota, R. Fukuda, J. Hasegawa, M. Ishida, T. Nakajima, Y. Honda, O. Kitao, H. Nakai, T. Vreven, J. A. Montgomery, Jr., J. E. Peralta, F. Ogliaro, M. Bearpark, J. J. Heyd, E. Brothers, K. N. Kudin, V. N. Staroverov, T. Keith, R. Kobayashi, J. Normand, K. Raghavachari, A. Rendell, J. C. Burant, S. S. Iyengar, J. Tomasi, M. Cossi, N. Rega, J. M. Millam, M. Klene, J. E. Knox, J. B. Cross, V. Bakken, C. Adamo, J. Jaramillo, R. Gomperts, R. E. Stratmann, O. Yazyev, A. J. Austin, R. Cammi, C. Pomelli, J. W. Ochterski, R. L. Martin, K. Morokuma, V. G. Zakrzewski, G. A. Voth, P. Salvador, J. J. Dannenberg, S. Dapprich, A. D. Daniels, O. Farkas, J. B. Foresman, J. V. Ortiz, J. Cioslowski, D. J. Fox. 2009, Gaussian 09, Gaussian, Inc., Wallingford CT.

[31] P. Henfeng. A non-covalent dimer formed in electrospray ionisation mass spectrometry behaving as a precursor for fragmentations. Rapid Commun Mass Spec. 2008, 22, 3555.

[32] C. Müller, B. Kanawati, T. M. Rock, S. Forcisi, F. Moritz, P. Schmitt-Kopplin. Dimer ion formation and intermolecular fragmentation of 1,2-diacylglycerols revealed by electrospray ionization Fourier transformion cyclotron resonance mass spectrometry for more comprehensive lipid analysis. Rapid Commun Mass Spec. 2014, 28, 1735.

[33] M. Sawada, Y. Okumura, H. Yamada, Y. Takai, S. Takahashi, T. Kaneda, K. Hirose, S. Misumi. Cross-chiral Examinations of Molecular Enantioselective Recognition by Fast Atom Bombardment Mass Spectrometry : Host-Guest Complexations Between Chiral Crown Ethers and Chiral Organic Ammonium Ions. Org. Mass. Spectrom. 1993, 28, 1525.

Legends for Schemes and Figures

Scheme 1.
The chemical structures of noscapine and hydrastine.

Fig. 1.
The MS/MS spectrum of the sodiated noscapine **1** (R,S) dimers.

Fig. 2.
The survival yield (SY) of the sodiated noscapine (a) and hydrastine (b) homodimers as a function of the collision energy. Figure insets show the zoomed survival yield versus collision energy curves in the range of 12.5 to 13.5 eV.

Fig. 3.
The MS/MS spectrum of the sodiated noscapine **3** (R,R)-L-tyrosine heterodimers.

Fig. 4.
The survival yield versus (SY) collision energy curves of the sodiated noscapine- L-tyrosine heterodimers. The figure inset shows the zoomed survival yield curves in the range of 5.5 to 6.5 eV.

Fig. 5.
The characteristic collision energy of the hydrastine **2** (S,R) and hydrastine **3** (R,R) mixtures as a function of the stereoisomeric excess (a) and the stereoisomeric purity (b), respectively.

Fig. 6.
The activation energy values of the fragmentation of noscapine **1** (R,S) and hydrastine **4** (S,S) homodimers as a function of the reciprocal of the ionic radius of the cation.

Fig. 7.
The calculated structures of the noscapine dimers cationized with the three different cations. a), b), and c) show the excised structures of the sodiated, potassiated and caesiated dimers, respectively

Table 1. The CE_{50} and the normalized CE_{50} values of the homodimers cationized with different alkaline metal cations

	CE_{50} (eV)			normalized CE_{50}		
	Na^+	K^+	Cs^+	Na^+	K^+	Cs^+
Noscapine 1 (R,S)	14.00	7.78	4.84	1.000	1.000	1.000
Noscapine 2 (S,R)	13.83	7.55	4.84	0.988	0.970	1.000
Noscapine 3 (R,R)	12.64	6.53	3.96	0.903	0.839	0.818
Noscapine 4 (S,S)	12.57	6.48	3.89	0.898	0.833	0.804
Hydrasitne 1 (R,S)	13.80	6.39	3.32	1.000	0.853	0.876
Hydrasitne 2 (S,R)	13.79	6.30	3.25	0.999	0.841	0.858
Hydrasitne 3 (R,R)	13.17	7.36	3.75	0.954	0.983	0.989
Hydrasitne 4 (S,S)	13.22	7.49	3.79	0.958	1.000	1.000

Table 2. The CE_{50} and the normalised CE_{50} values of the sodiated heterodimers

	CE_{50} (eV)				normalized CE_{50}			
	L-Lys	D-Lys	L-Tyr	D-Tyr	L-Lys	D-Lys	L-Tyr	D-Tyr
Noscapine **1** (R,S)	5.64	5.40	5.37	5.06	1.000	0.956	1.000	0.967
Noscapine **2** (S,R)	5.41	5.65	4.88	5.23	0.959	1.000	0.909	1.000
Noscapine **3** (R,R)	4.75	4.95	3.95	4.38	0.842	0.876	0.736	0.837
Noscapine **4** (S,S)	4.85	4.63	4.34	3.91	0.860	0.819	0.808	0.748
Hydrasitne **1** (R,S)	6.88	6.70	6.78	6.38	1.000	0.977	1.000	0.973
Hydrasitne **2** (S,R)	6.68	6.86	6.47	6.56	0.971	1.000	0.954	1.000
Hydrasitne **3** (R,R)	5.19	5.32	3.94	4.34	0.754	0.776	0.581	0.662
Hydrasitne **4** (S,S)	5.35	5.16	4.46	4.12	0.778	0.752	0.658	0.628

Table 3. The composition of the test solutions and the measured and calculated stereoisomeric purity of hydrastine **2** (S,R).

Composition (%)				
Hydrastine 2 (S,R)	**Hydrastine 3 (R,R)**	**ep% hydrastine 2 calculated (%)**	**ep% hydrastine 2 measured (%)**	**standard deviation**
70	30	70.0	73.2	0.440
10	90	10.0	11.7	0.915
50	50	50.0	52.4	0.681

Table 4. The slopes, the intercepts and the correlation coefficients (R^2) of the linear trend lines of the CE_{50} *versus* reciprocal ionic radius of the ionizing cations (Na^+, K^+, and Cs^+) for the noscapine and hydrastine homodimers.

	slope	intercept	R^2
Noscapine **1**	2.41	-9.64	1.000
Noscapine **2**	2.38	-9.49	0.999
Noscapine **3**	2.30	-9.86	0.999
Noscapine **4**	2.23	-9.95	0.999
Hydrastine **1**	2.77	-13.34	1.000
Hydrastine **2**	2.81	-13.65	1.000
Hydrastine **3**	2.45	-10.67	0.994
Hydrastine **4**	2.45	-10.64	0.994

Table 5. The calculated Gibbs free energies and the activation energies of the fragmentation of the dimers ($[2M+Cat]^+$)

	Calculated Gibbs free energy (eV)		Activation energy of the fragmentation (eV)	
	Noscapine **1**	Noscapine **4**	Noscapine **1**	Noscapine **4**
Na^+	0.75	0.74	0.71	0.67
K^+	0.36	0.30	0.54	0.51
Cs^+	0.29	0.27	0.47	0.46

Scheme 1

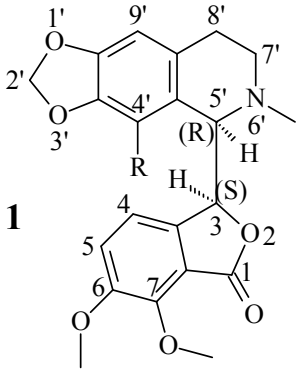

1

R: OMe (-)-alpha-noscapine
R: H (-)-beta-hydrastine

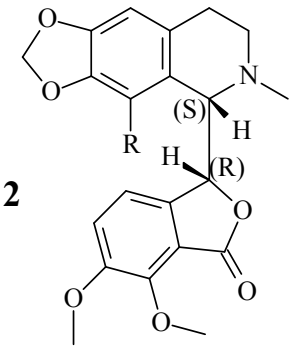

2

R: OMe (+)-alpha-noscapine
R: H (+)-beta-hydrastine

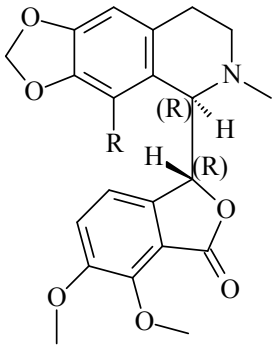

3

R: OMe (-)-beta-noscapine
R: H (-)-alpha-hydrastine

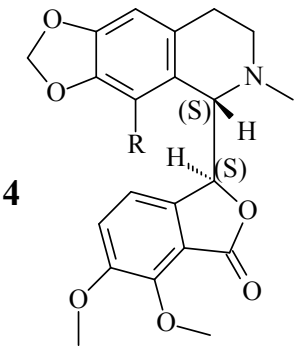

4

R: OMe (+)-beta-noscapine
R: H (+)-alpha-hydrastine

Fig 1

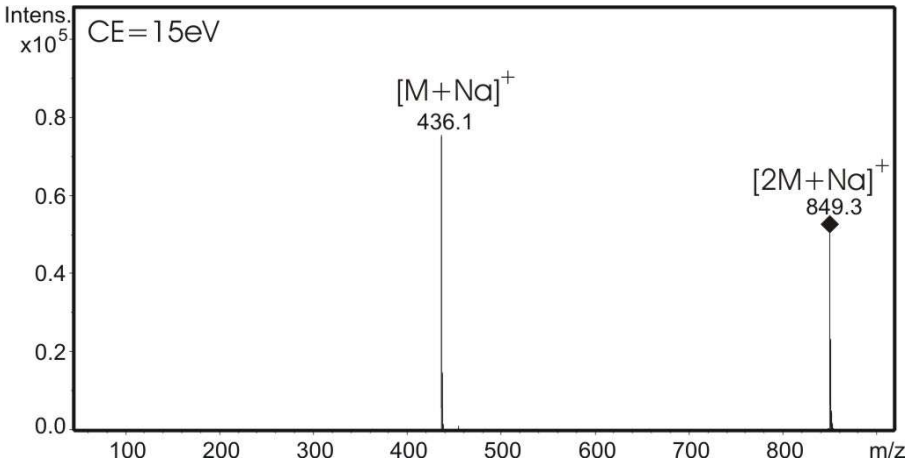
Intens.
x10^5
CE=15eV
[M+Na]+
436.1
[2M+Na]+
849.3
0.0
0.2
0.4
0.6
0.8
100
200
300
400
500
600
700
800
m/z

Fig 2

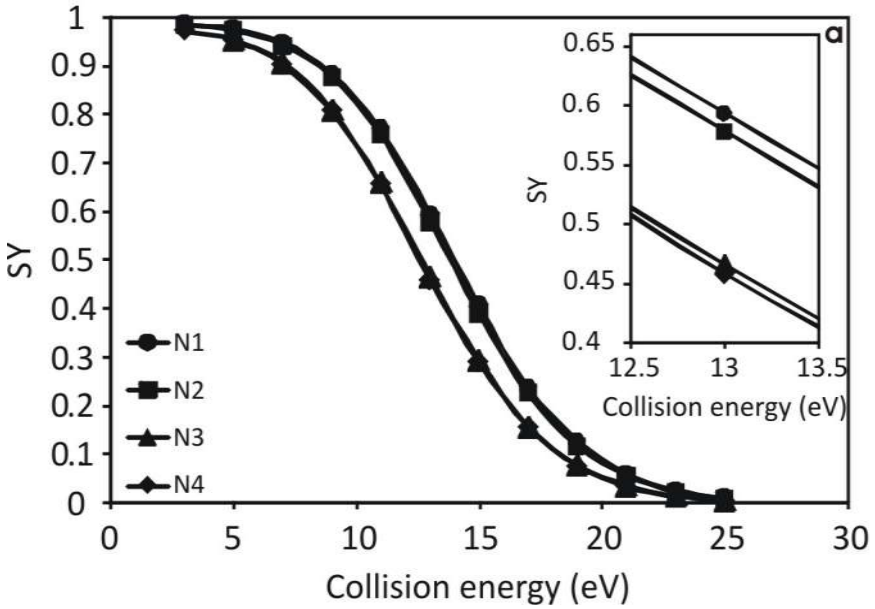
a
SY
Collision energy (eV)
N1
N2
N3
N4

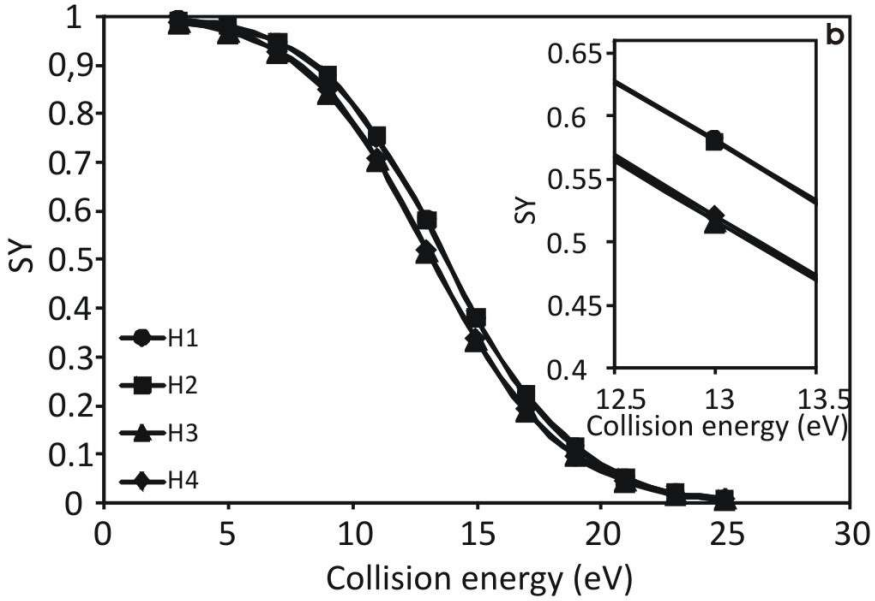
b
SY
Collision energy (eV)
H1
H2
H3
H4

Fig 3

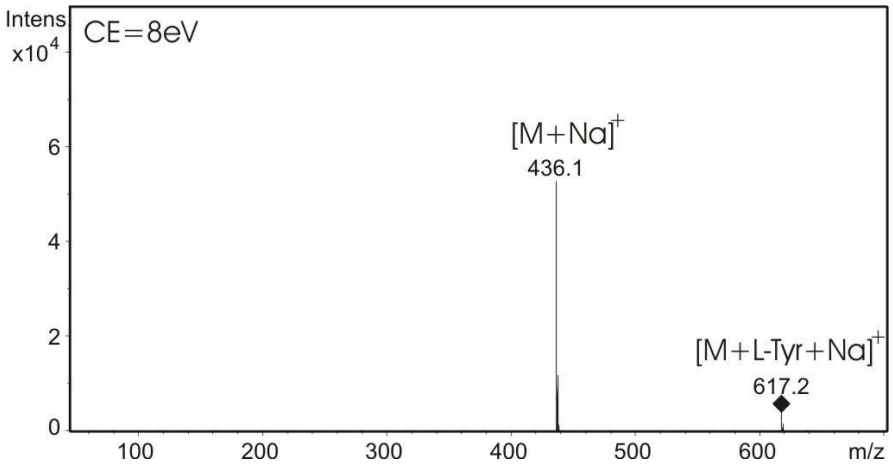
Intens
x10^4
CE=8eV
[M+Na]+
436.1
[M+L-Tyr+Na]+
617.2
m/z

Fig 4

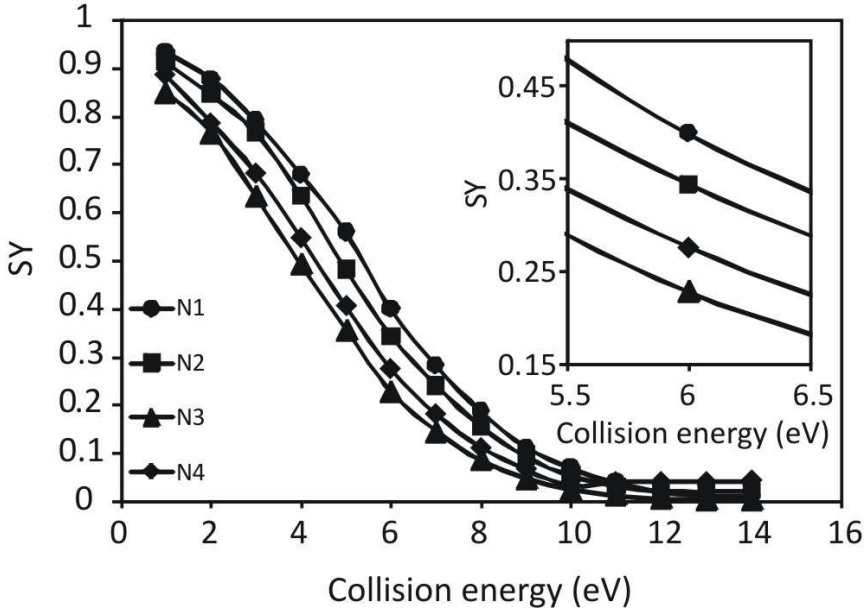
SY
N1
N2
N3
N4
Collision energy (eV)
SY
Collision energy (eV)

Fig 5

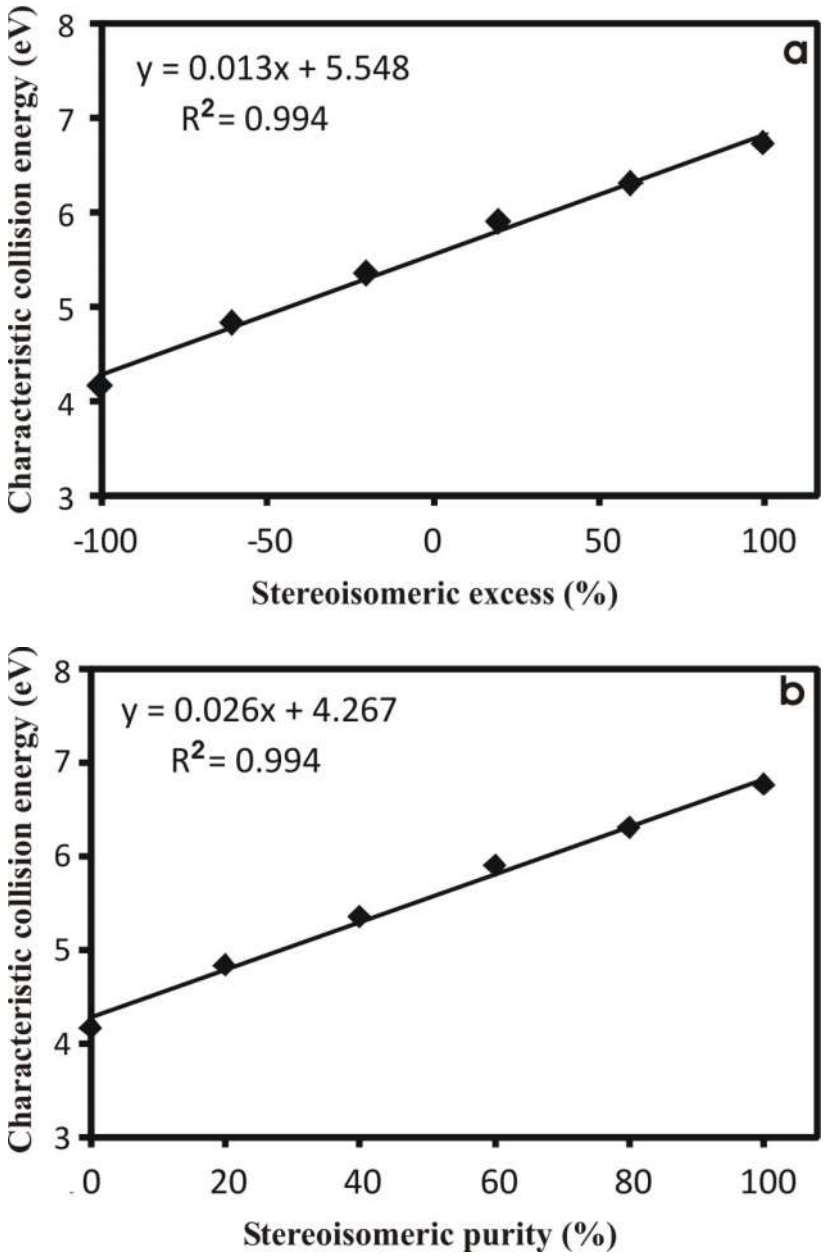
a
y = 0.013x + 5.548
R2= 0.994
Characteristic collision energy (eV)
Stereoisomeric excess (%)
b
y = 0.026x + 4.267
R2= 0.994
Characteristic collision energy (eV)
Stereoisomeric purity (%)

Fig 6

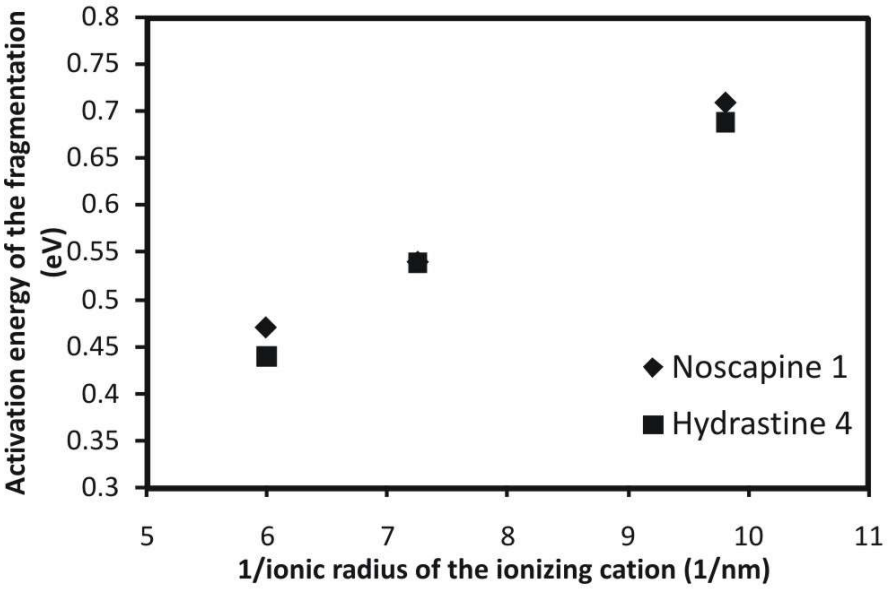
Activation energy of the fragmentation (eV)
0.8
0.75
0.7
0.65
0.6
0.55
0.5
0.45
0.4
0.35
0.3
5
6
7
8
9
10
11
1/ionic radius of the ionizing cation (1/nm)
Noscapine 1
Hydrastine 4

Fig 7

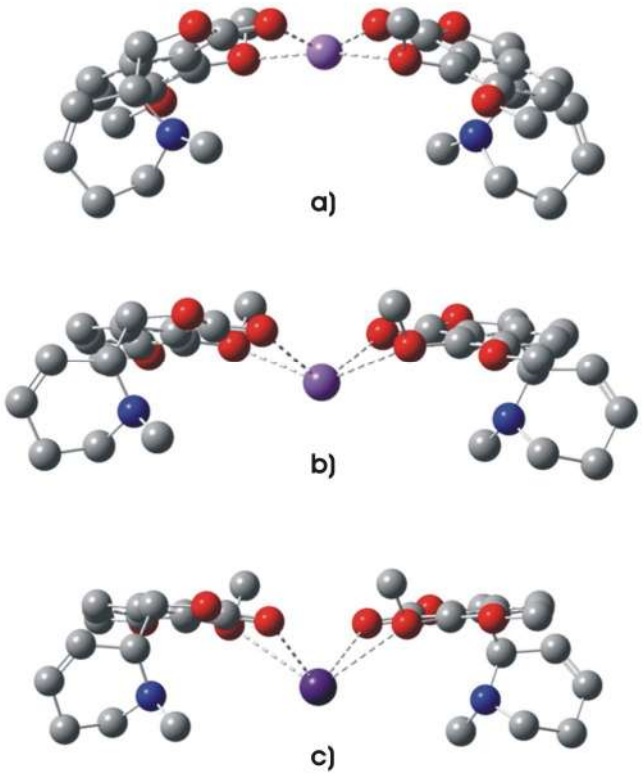
a)
b)
c)